Available online at BCREC website: https://bcrec.id

Bulletin of Chemical Reaction Engineering & Catalysis, 17 (2) 2022, 466-475

Research Article

Photodegradation of Rhodamine-B Dye under Natural Sunlight using CdO

Dipali Lavate*, Vikas Sawant, Ashok Khomane

Department of Chemistry, Rajaram college, Kolhapur 416004, India.

Received: 3rd May 2022; Revised: 12th June 2022; Accepted: 13th June 2022
Available online: 14th June 2022; Published regularly: June 2022

Abstract

The present study includes synthesis of CdO thin film by simple and cost effective chemical bath deposition method. Cadmium monochloroaceatate were used for preparation of CdO thin film. The structural, optical properties of CdO thin film were investigated with the help of X-ray diffraction (XRD) and UV-Vis NIR double beam spectrometry. The XRD studies revealed that annealed thin film shows crystalline in nature having 48.4 nm in size. The optical band gap of thin film was found to be 2.13 eV. Scanning Electron Microscopy (SEM) images shows sphere like structure which is closely arranged with each other. The presence of functional group was confirmed by Fourier Transform Infra Red (FTIR). Brunauer–Emmett–Teller (BET) surface area analysis confirm formation of a mesoporous CdO with 6.01 m^2/g surface area and 31.96 nm average pore diameter. The photocatalytic activity of prepared thin film was checked by using Rhodamine-B as a model dye under natural sunlight and found to be 48%.

Keywords: Thin film; Chemical bath deposition; Optical properties; Photocatalytic activity; Rhodamine-B

How to Cite: D. Lavate, V. Sawant, A. Khomane (2022). Photodegradation of Rhodamine-B Dye under Natural Sunlight using CdO. *Bulletin of Chemical Reaction Engineering & Catalysis*, 17(2), 466-475 (doi:10.9767/bcrec.17.2.14172.466-475)

Permalink/DOI: https://doi.org/10.9767/bcrec.17.2.14172.466-475

1. Introduction

Now a day, photocatalysis has received more attention all over the world because water pollution from different industries is a major issue. Many synthetic dyes are used as coloring agent in various industries like leather, textile, food, cosmetics and other industries. These industries have released dye pollutants as a waste water in the environment. Thus dye pollutant is a major source of water pollution, because the effluent from textile industry contains large number of toxic, carcinogenic, non-biodegradable organic dye compounds [1,2]. Thus wastewater contain dye pollutant from textile industry creates many series problem to humans, animals and environment. Hence water treatment as becomes major issue of society therefore, water purification was a lot gain attention.

Various physicochemical and biological methods like filtration, flocculation, coagulation, adsorption, ozonisation, activated sludge processes and photocatalytic degradation are used for treatment of waste water [3–6]. Out of these techniques, photocatalytic degradation of dyes for waste water treatment as attracted much more attention due to easy operation, effectiveness, and producing non toxic end products. Photocatalysis is based on the absorption of light by the semiconductor catalyst. Electrons are excited from lower energy to higher energy band, leading to the formation of electron hole pairs. Now a day, well efforts have been take to develop metal oxide semiconductor materials with narrow band gap for increasing photocata-

* Corresponding Author.
Email: dipalilavate65@gmail.com (D. Lavate);

lytic activity under solar light during photocatalysis. Various photocatalyst, such as titanium oxide (TiO_2), LDHs-based catalysts, zirconia (ZrO_2), calcium oxide (CaO), niobium pentaoxide (Nb_2O_5), iron(III) oxide (Fe_2O_3), molybdenum oxide (MoO_3), Fe@MWCNT, and Z-scheme photocatalysts are used for the treatment of waste water [7–11]. Wang *et al.* [12] designed CdO/CdS HT to improve the photocatalytic performance of CdO and CdS MLs.

Cadmium oxide (CdO) is an *n*-type semiconductor with a direct band gap energy of 2.2 eV and an indirect band gap energy of 1.36–1.98 eV [13]. High electrical conductivity with a moderate refractive index makes it a constructive material for various applications such as solar cells, gas sensors, photovoltaic, optoelectronic, and photosensors [13,14]. Its band gap is tailored to the absorption of the visible region of sunlight and therefore it shows a photocatalytic mechanism similar to that of other semiconductor oxides. Thus, cadmium oxide shows selective photocatalytic properties that make the compound suitable for the degradation of toxic compounds like dyes, pigments, and environmental pollution [15].

Various techniques are used to obtain CdO in the form of film or powder, such as solvothermal method [16], chemical vapour deposition [17], sol-gel method [18], spray pyrolysis [19], sputtering [20]. Use of these methods is limited because of some technical issues like high cost, complicated apparatuses, long reaction time, and so on. Despite these difficulties, for the fabrication of CdO thin films, chemical bath deposition method is used [21]. Chemical bath deposition (CBD) is a very simple and low cost method. Less material wastage and no need to handle poisonous gases are additional advantages of this method. In the present investigation, we have selected chemical bath deposition method for the preparation of CdO.

The novelty of our research work is the synthesis of CdO using cadmium monochloroaceatate for the first time. Prepared material was characterized by using XRD, EDX, UV-visible, and FTIR. The photocatalytic activity of CdO was checked by using Rhodamine-B dye solution under sunlight.

2. Materials and Methods

The A.R. grade chemicals, such as cadmium carbonate ($CdCO_3$), monochloroacetic acid ($ClCH_2COOH$), sodium hydroxide (NaOH), and ammonia (NH_3), were used for the synthesis of CdO. The glass plates with dimensions 75×26 mm were used for the deposition of CdO thin film sample. The glass plates were washed in chromic acid, alcohol, and distilled water before the deposition of the film sample [22]. For that, the solution of 0.25 M cadmium monochloro acetate was prepared by dissolving cadmium carbonate in an equivalent solution of 0.25 M monochloroacetic acid solution (pKa = 1.25 at 25 °C) with constant stirring. In the above solution, 5 mL 2 M NaOH and 5 mL of 1:1 NH_3 solution were added from the burette. Then, the whole reaction mixture was diluted to 50 ml by adding distilled water and heated at 80 °C for 90 min. Cleaned dry glass substrates were vertically immersed in bath and heated at about 80 °C for 2 h. The obtained film was washed with deionised water several times, dried and kept in electric oven at 200 °C and 400 °C for 3 h to obtain CdO. The chemical reaction mechanism for the preparation of CdO is represented as follows:

$$CdCO_3 + 2(ClCH_2COOH) \rightarrow (ClCH_2COO)_2Cd + CO_2 + H_2O \quad (1)$$

$$(ClCH_2COO)_2Cd + 2NH_4OH \rightarrow Cd(OH)_2 + (ClCH_2COO)_2(NH_4)_2 \quad (2)$$

$$Cd(OH)_2 \rightarrow CdO + H_2O \quad (3)$$

2.1 Material Characterizations

The structural properties of prepared CdO thin films were investigated by X-ray diffraction (XRD) using Cu-Kα radiation having wavelength 1.5415 Å at an operating voltage of 40 kV and current for X-ray gun as 40 mA. For surface morphological analysis JEOL JSM-6360, Japan Scanning Electron Microscope (SEM) was used. EDX analysis techniques were used for compositional analysis of CdO thin film. The UV visible spectrometer was used to measure a optical absorption. For the investigation of surface area and average pore diameter of CdO material BET surface analyzer (Lab India) were used. The diffused reflectance spectra were recorded on UV-visible NIR double beam spectrometer (JASCO,V-770). The FTIR spectrometer (JASCO, 4600 JAPAN) was used for FTIR spectral analysis. The photocatalytic activity of CdO was studied by the time dependent counting of absorption data under visible region on UV-Vis-NIR double beam spectrometer (Shimadzu UV 310 PC).

2.2 Photocatalytic Study

The photocatalytic activity of prepared CdO thin films was investigated by determining photodegradation of Rhodamine-B dye under natural sunlight irradiation. In photocatalytic

experiments, 100 mL 10 ppm Rhodamine-B dye solutions were taken in 100 mL glass beaker containing CdO thin film as a photocatalyst. Then, the solution was kept in the dark for at least 1 h to attain adsorption/desorption equilibrium. After adsorption/desorption equilibrium solution was kept under sunlight of average intensity of 6.66 kwh/m²/day (Latitude: 16.75 longitude: 74.25). First sample was taken before the irradiation, which was considered as the initial concentration ($A_{initial}$). After a regular time interval of irradiation (30 min) solution was taken and analyzed by using a UV-vis-NIR spectrophotometer at wavelength range from 400 to 800 nm and the value of 150 min was taken (A_{final}). The efficiency of material was calculated by using following Equation (4) [23,24].

$$Efficiency\ (\%) = \frac{A_0 - A_t}{A_0} \times 100 \quad (4)$$

where, A_0 is initial absorbance, and A_t is absorbance after t time reaction.

3. Results and Discussions

3.1 XRD Analysis

Figure 1 and Figure 2 show XRD pattern of CdO annealed at 200 °C and 400 °C, respectively. The CdO sample annealed at 200 °C shows low intensity of peak due to partial crystalline nature as shown in Figure 1. Meanwhile, annealed at 400 °C shows high intensity of peak due to total conversion of partial amorphous sample into crystalline nature as shown in Figure 2. The peaks of CdO annealed at 400 °C are observed at 33.10°, 38.56°, 55.32°, 66.25°, 69.52°, respectively and indexed to the (111), (200), (220), (311), (222) planes, respectively, which coincide well with the JCPDS data (JCPDS Data file no.00-001-1049). The observed d value corresponds to cubic structure of CdO. The crystallographic lattice parameters of CdO were determined by following Equation (5).

$$\frac{1}{d^2} = \frac{h^2 + k^2 + l^2}{a^2} \quad (5)$$

The lattice parameters 'a' values are very close to the standard value of CdO and were found to be 4.6846 Å at 400 °C as shown in Table 1. The crystalline size estimated using the higher intensity peak of plane the (111) was 48.4 nm.

3.2 Scanning Electron Microscope (SEM) and Energy Dispersive X-ray (EDX) Analyses

Scanning Electron Microscope is used for morphological study. SEM images of CdO sample is as shown in Figure 3. It shows a sphere

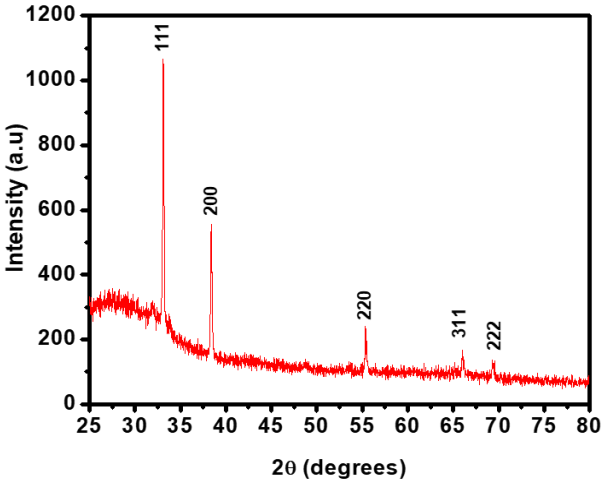

Figure 1. XRD pattern of CdO annealed at 200 °C.

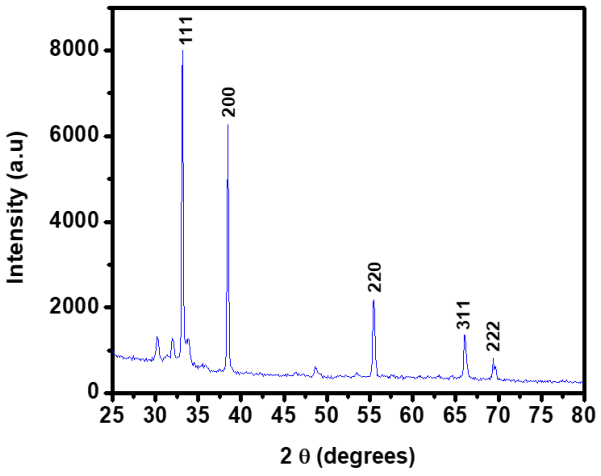

Figure 2. XRD pattern of CdO annealed at 400 °C.

Table 1. Crystallographic parameters of CdO thin film annealed at 400 °C.

Material	*d* values Å cubic		*hkl* plane	Lattice parameter (Å)	Crystalline size
	Standard	Observed			
CdO	2.70000	2.70414	111	a=4.6846	D = 48.4 nm
	2.34000	2.33387	200		
	1.65000	1.65928	220		
	1.41000	1.40956	311		
	1.35000	1.35103	222		

like structure, which is closely arranged with each other, responsible for increase in catalytic efficiency. The catalytic efficiency increases due to increase in surface area. Energy dispersive X-ray analyses were used for the determination of elemental composition. The EDX of CdO is as shown in Figure 4. From the figure, it is clear that the formation of CdO takes place and it does not contain any impurity. The spectrum shows the weight percentage of Cd and O was found to be 75.19% and 24.81%.

3.3 Optical Studies

Band gap energy of a photocatalyst is one of the most important parameters for selection of light sources, which is used to excite the electron from the valence band (VB) to the conduction band (CB) and generate electron–hole pair (e^-–h^+) and thereby degrade the dyes [25].

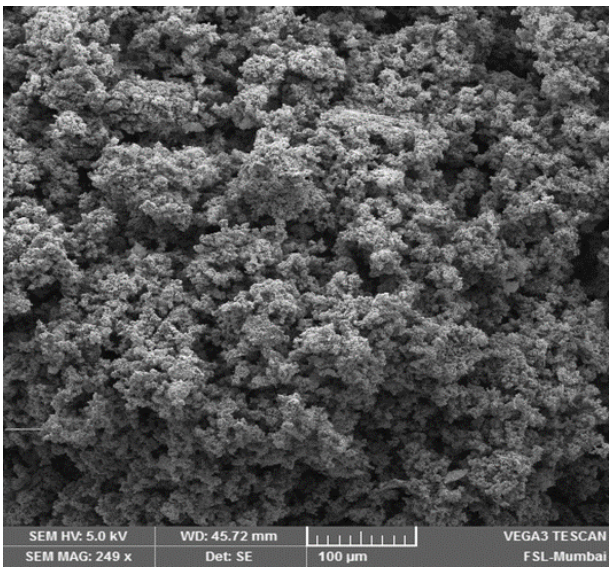

Figure 3 .SEM image of CdO annealed at 400 °C.

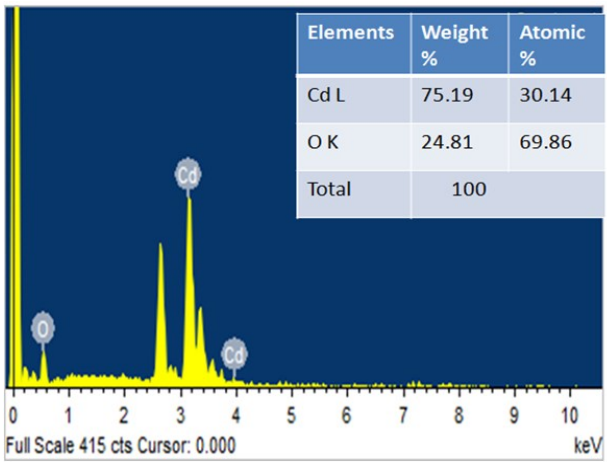

Figure 4 .EDX analysis of CdO annealed at 400 °C.

The plot of absorbance as a function of wavelength in the range from 350–800 nm for the CdO sample is shown in Figure 5(a). It reveals the absorption edge was found at 580 nm wavelengths A similar absorption band spectra were observed by Bulakhe *et al.* [26] using a wet chemical method. The band gap energy is determined by the following Equation (6) [27],

$$(\alpha h\upsilon) = B\left(h\upsilon - E_g\right)^n \quad (6)$$

where, $h\upsilon$ = photon energy, α = absorption coefficient, B = constant value and E_g = band gap energy. The band gap energy of the prepared sample can be determined by plotting $(\alpha h\upsilon)^2$ vs $h\upsilon$ and obtaining the extrapolation of this curve as shown in Figure 5(b). The band gap energy of the prepared CdO is 2.13 eV, which is matched with previous report [26,28]. The optical band gap value was reduced due to its more crystalline structure (as is seen from XRD) and transition between the partially forbidden

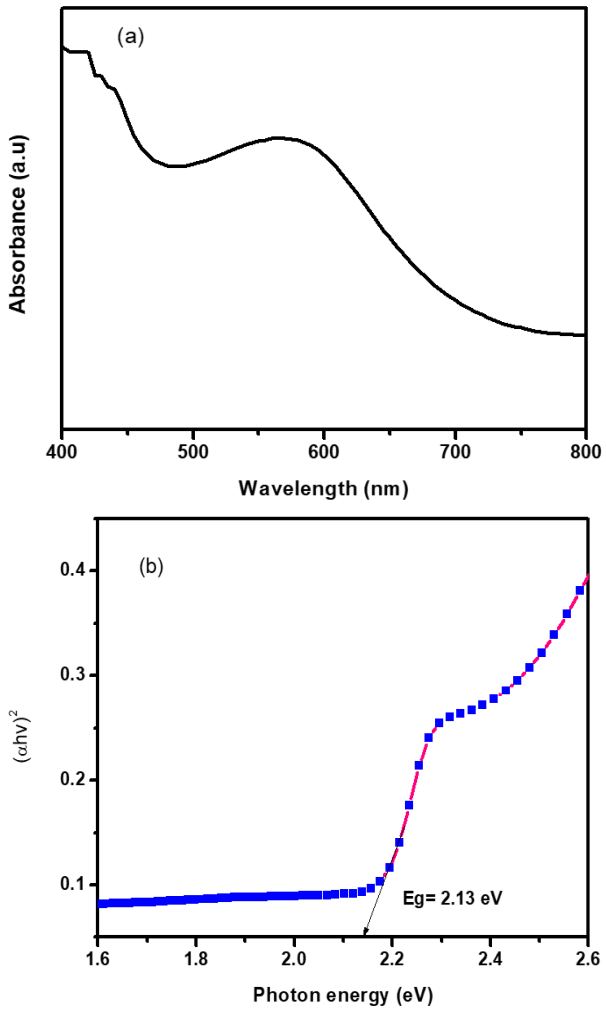

Figure 5. (a) The plot of absorbance with respect to wavelength for CdO, (b) Optical band gap calculation of CdO.

valence band and conduction band of *d*-shell electrons of cadmium ions [29].

3.4 FTIR Studies

The Fourier Transform Infrared Spectroscopy (FTIR) is used to identify the functional group presents in prepared samples, which are recorded in the range of 400–4000 cm^{-1}. Figure 6 shows FTIR spectra of prepared samples. The strong absorption peak at 3444 cm^{-1} is due to the O–H group in water molecules [30]. The peak at 2916 cm^{-1} is due to C–H symmetric stretching vibration. The peak at 1029 cm^{-1} is due to C–O stretching vibration of absorbed CO_2 [31]. Meanwhile, bands in the range of 400–700 cm^{-1} correspond to Cd–O mode of vibration [32].

3.5 BET and BJH Analyses

The Figure 7 shows the adsorption-desorption isotherm of CdO. The nature of graph is Type IV isotherm with hysteresis loop, which revealed the mesoporous nature of CdO. The Figure 8 shows the Barret-Joyner-Halenda (BJH) pore size distribution. The CdO has a surface area of 6.01 m^2/g. The peak in BJH shows the average pore diameter 31.96 (nm).

3.6 Photocatalytic Activity of CdO

The Figure 9 shows typical absorbance characteristics of Rhodamine-B solution degraded by CdO thin film. The characteristics absorption peak of Rhodamine-B dye at 553 nm is used to monitor the photocatalytic degradation process. The colour of dispersed solution disappeared after 30 min and the main absorption peak of Rhodamine-B at 553 nm disappeared and the intensity of the peak decreased. CdO photocatalyst has about 48% degradation efficiency of Rhodamine-B dye at 150 minutes. The photocatalytic activity of the CdO photocatalyst in comparison with other photocata-

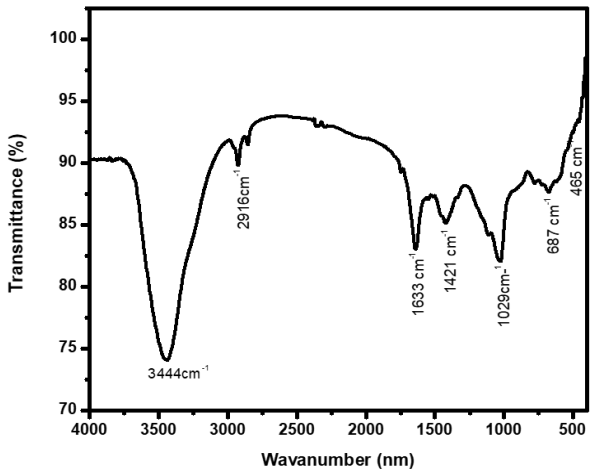

Figure 6. Shows the FTIR spectrum of chemical bath deposited CdO.

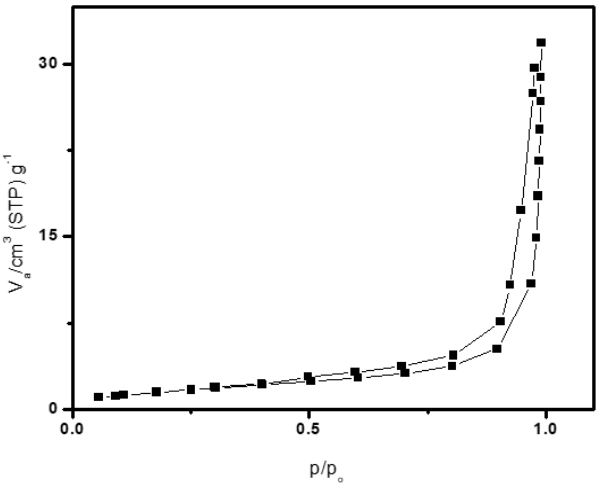

Figure 7. N_2 adsorption desorption of CdO.

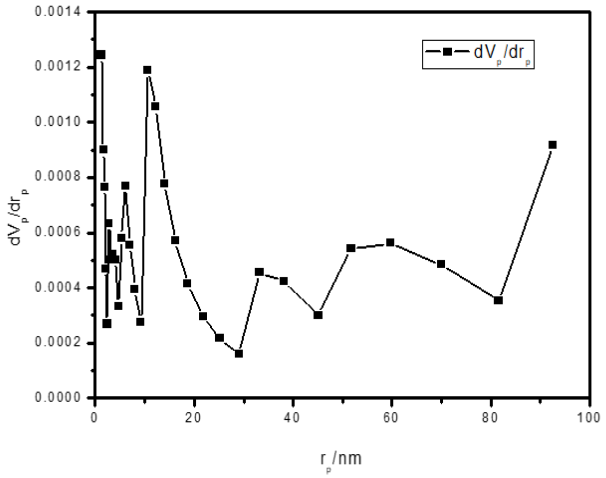

Figure 8. Pore size distribution of CdO.

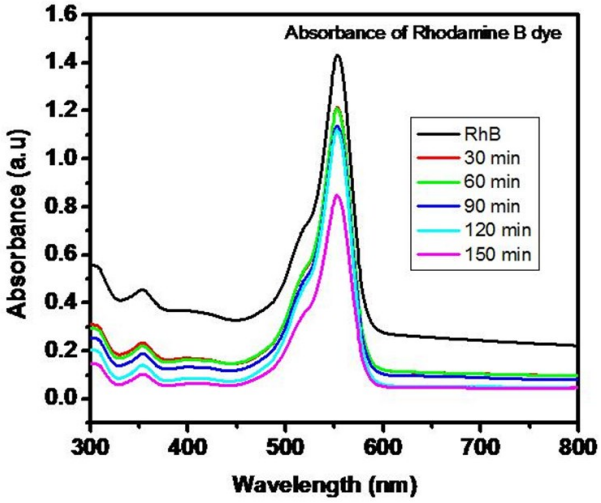

Figure 9. Absorbance spectra of Rhodamine B dye.

lyst is summarized in Table 2. The photocatalytic efficiency of CdO is increased due to a high degree of crystallization which is revealed in XRD results. The rate of reaction could be detected by studying the absorbance data $\ln(C_0/C_t)$ with respect to the reaction time as shown in Figure 10(b), where C_0 and C_t are the concentrations of Rhodamine-B at the initial stage and time (t), respectively (Figure 10(a)). A pseudo first order kinetics was observed and the calculated rate constant was found to be 3.51×10^{-3} min^{-1} [36].

pH plays an important role in the photocatalytic study, because it controls the reaction during the photodegradation of dye. The effect of pH on photodegradation efficiency was studied by varying the pH from 2 to 10 using HCl and NaOH and result is presented in Figure 11. The minimum degradation efficiency was observed at pH 2 to 6 and maximum at pH 10. The pH mostly affects the surface properties of CdO, dissociation of dye molecule and formation of hydroxyl radicals [37].

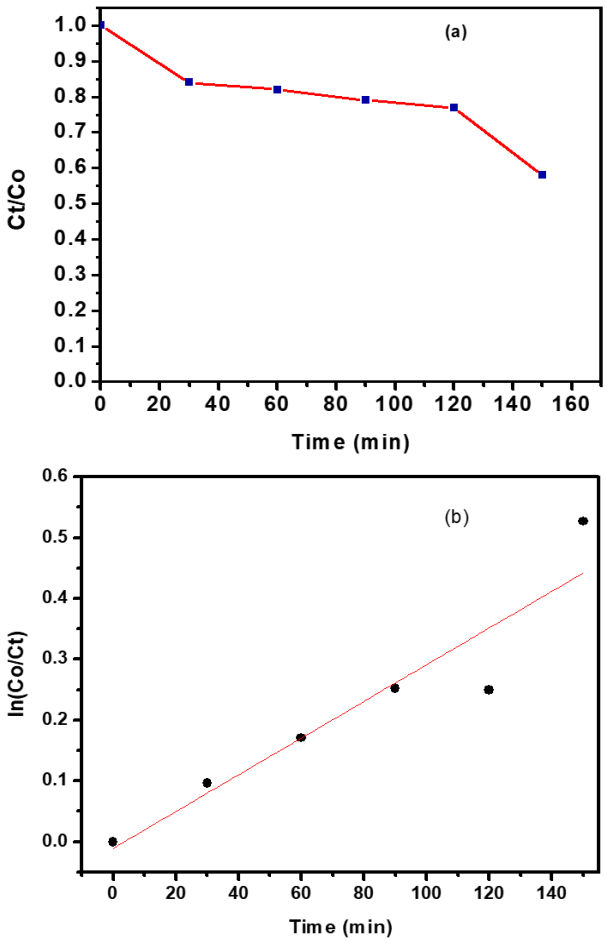

Figure 10. (a) Photocatalytic degradation of RhB dye over time, (b) Kinetic study for photodegradation of RhB using CdO.

3.7 FTIR Study of Rhodamine-B

The functional group of Rhodamine-B was investigated by using FTIR spectroscopy. The peaks at 1585.04 cm^{-1} and 1407.21 cm^{-1} are attributed to aromatic carbon ring vibration while the peak at 1338.43 cm^{-1} is due to carbon-aryl bond vibration .The peak attributed to alkyl chloride group at 1175 cm^{-1}, asymmetric stretching of carbon–oxygen-carbon ether bond at 1067.48 cm^{-1}, 1004.92 cm^{-1}, and bending vibration of aromatic hydrogen at 680.71 cm^{-1}. The transmission against wavenumber graph is as shown in Figure 12. When Rhodamine-B dye and CdO mixture is irradiated with the sunlight for 150 min then transmission of same was also measured against wavenumber does not shows any peak which confirm that degradation of Rhodamine-B dye by using sunlight.

3.8 Photodegradation of Rhodamine-B Dye Mechanism using CdO

Schematic diagram of photocatalytic degradation of mechanism of Rhodamine-B dye us-

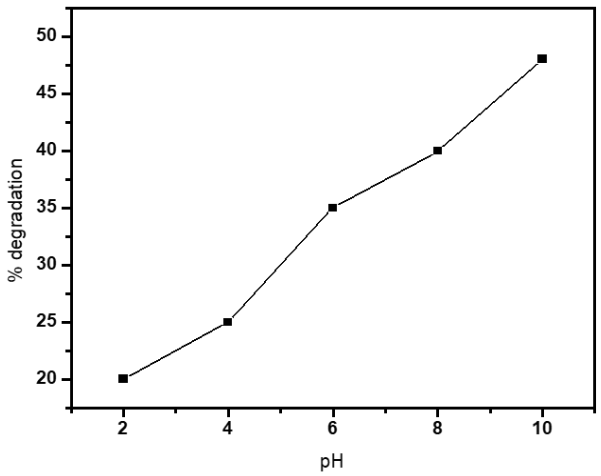

Figure 11. Effect of pH against % degradation of RhB dye under sunlight irradiation.

Table 2. Comparison of Rhodamine-B dye degradation by using various photocatalyst.

Photocatalyst	Dye	Irradiation source	Degradation (%)	Time	Reference
CdO	RhB	Sunlight	48	180 min	This work
C doped TiO_2	RhB	500 W tungsten halogen lamp	59	5 h	[33]
Co_3O_4	RhB	Visible light	32	180 min	[34]
Mn/Fe-MOF	RhB	Visible Light	-	-	[35]

ing CdO is shown in Figure 13. CdO irradiated with sunlight, electrons are excited from the valence band (VB) to the conduction band (CB) resulting in the formation of positively charged holes (h^+_{VB}) and negatively charged electrons (e^-_{CB}) on the surface of CdO.

$$CdO + \text{sunlight} \rightarrow CdO\ (h^+_{VB} + e^-_{CB}) \quad (7)$$

Recombination of electron-hole pairs is possible in volume and surface of the photo catalysts. On the other, and when electron -hole pairs migrate to the surface of CdO, they can participate in redox reaction with the adsorbed species. During a redox reaction, a hydroxyl radical is formed by interaction of a hole with the adsorbed surface group, while electrons react with oxygen to form a superoxide radical ($\cdot O_2^-$).

The negatively charged electrons in the conduction band react with O_2 molecule and H^+ (surrounding the aqueous environment) and gather hydrogen peroxide, which supplies OH^- and $\cdot OH$ free radical, which can further react

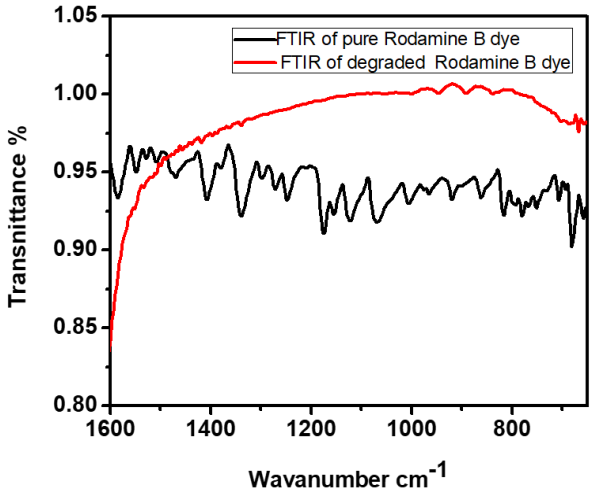

Figure 12. FTIR spectrum of photodegraded of Rhodamine-B dye.

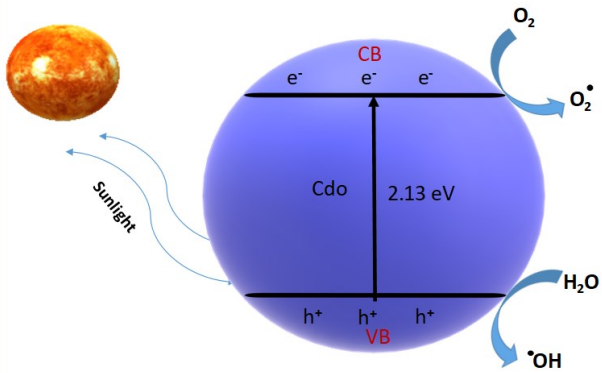

Figure 13. Mechanism on the photodegradation of Rhodamine-B using CdO.

to form hydrogen peroxide and other active oxygen radicals. Highly reactive free radicals, which break the organic compounds into water and carbon dioxide. The photodegradation reaction of Rhodamine-B using CdO photocatalyst is shown in Equations (8-12).

$$h^+_{VB} + OH^- \rightarrow \cdot OH \quad (8)$$
$$e^-_{CB} + O_2 \rightarrow \cdot O_2^- \quad (9)$$
$$O_2 + 2\ e^- + 2H^+ \rightarrow H_2O_2 \quad (10)$$
$$H_2O_2 + \cdot O_2^- \rightarrow OH^- + \cdot OH + O_2 \quad (11)$$
$$\cdot OH + \text{Rhodamine B} \rightarrow \text{Degradation products} \quad (12)$$

Thus, on the surface of CdO photocatalyst oxidation and reduction reaction occurs, from the time when this reaction produces positive holes and negative electrons. In oxidation reaction moisture contents in the CdO surfaces reacts with hole and return free hydroxyl radical. If more amount of oxygen is provided, this acts as an electron acceptor and recombination rate is delayed which further enhances degradation of pollutants.

The electrons and holes diffuse to the surface of CdO in which they can be utilized for various redox processes. The superoxide radical ($\cdot O_2^-$) if formed by reaction of negative electron with oxygen, positive hole reacts with water to form powerful oxidizing free radicals and perform similar oxidative attack on Rhodamine-B dye [38,39].

During the photodegradation of Rhodamine-B dye process, different active species as holes (h^+), hydroxyl radical ($\cdot OH$), superoxide radicals ($\cdot O_2^-$) and electrons (e^-) are mainly generated. To detect the main reactive species that responsible for the photodegradation of Rhoda-

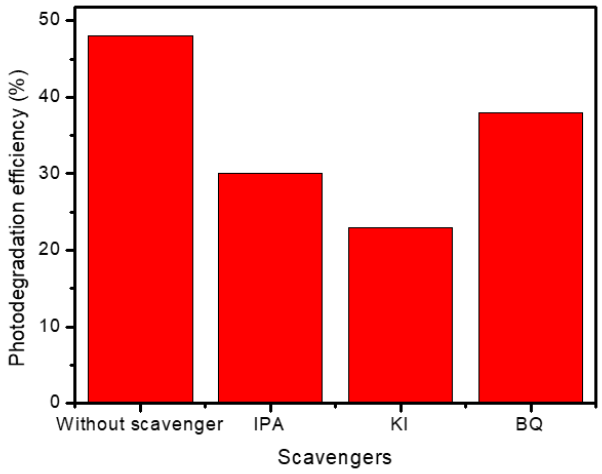

Figure 14. Scavenger test on the photodegradation efficiency of CdO thin film (annealed at 400 °C) in degrading RhB solution.

mine-B dye under natural sunlight irradiation, scavenger tests were investigated. Generally, electrons have negligible effect on photodegradation of organic pollutant [40] and thus electron scavenger test was excluded. Three different scavengers, such as isopropanol (IPA), potassium iodide (KI) and benzoquinone (BQ), were used as $\cdot OH$, h^+ and $\cdot O_2^-$ scavengers, respectively [41].

The effect of scavengers on the photodegradation of Rhodamine-B dye using CdO thin film is shown in Figure 14. It concluded that, the photodegradation efficiency of CdO thin film without scavenger was 48 % after 150 min under sunlight irradiation. A slight decrease in photodegradation efficiency of Rhodamine-B dye was observed when IPA and BQ were used as $\cdot OH$ and $\cdot O_2^-$ quenchers which indicates that $\cdot OH$ is more significant compared to $\cdot O_2^-$ in degradation process of Rhodamine-B dye. However, a drastic decrease in the degradation efficiency was observed when KI were used as h^+ scavengers which indicates that h^+ are the main reactive species in the degradation of Rhodamine-B over CdO under sunlight irradiation.

In order to find the reusability and stability of the photocatalyst, the CdO thin film was further used under the same experimental conditions. Five cycles have been carried out for CdO thin films used for photocatalysis. Between each cycle films are taken out, washed with distilled water and dried. It is evaluated that photocatalytic activity of thin film is not much affected. Figure 15 shows the results of five cyclic run for RhB degradation over CdO. In fifth cycle photodegradation reached to 45%, which is only 3% lower than that of first cycle.

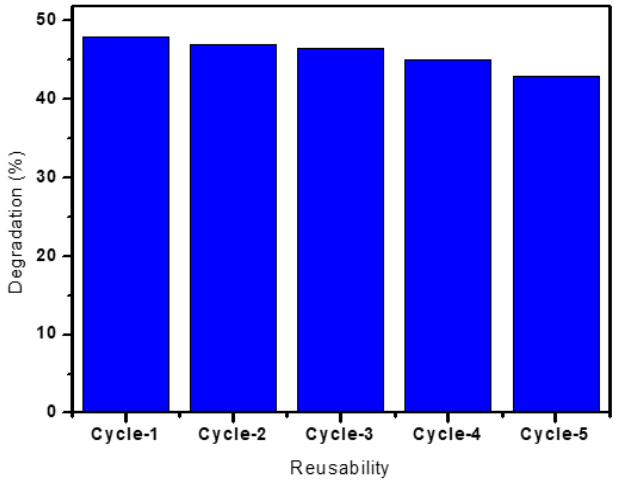

Figure 15. Photocatalyst reusability test.

4. Conclusions

CdO thin film have been grown successfully onto glass substrates via a simple chemical bath deposition method (CBD). The XRD studies revealed that annealed thin film shows crystalline in nature having 48.4 nm in size. CdO thin films have optical band gap of 2.13 eV. This study indicated that the CdO thin film can be used as a suitable photocatalyst to remove the Rhodamine-B dyes. High degree of crystallization, small size and low band gap are responsible for excellent photocatalytic efficiency of CdO under natural sunlight.

Acknowledgment

The author gratefully acknowledges the principle Dr. A. S. Khemnar, Rajaram college, Kolhapur for his constant encouragement and cooperation in the research activity.

References

[1] Forgacs, E., Cserha, T., Oros, G. (2004). Removal of synthetic dyes from wastewaters: a review. *Environment International,* 30, 953. DOI: 10.1016/j.envint.2004.02.001

[2] Zhu, H.Y., Fu, Y.Q., Jiang, R., Jiang, J.H., Xiao, L., Zeng, G.M., Zhao, S.L., Wang, Y. (2011). Adsorption removal of congo red onto magnetic cellulose/Fe_3O_4/activated carbon composite: Equilibrium, kinetic and thermodynamic studies. *Chemical Engineering Journal,* 173, 494. DOI: 10.1016/j.cej.2011.08.020

[3] Verma, A.K., Dash, R., Bhunia, P. (2012). A review on chemical coagulation/flocculation technologies for removal of colour from textile wastewaters. *Journal of Environmental Management*, 93, 154. 10.1016/j.jenvman.2011.09.012

[4] Cheng, S.H., Oatley, D.L., Williams, P.M., Wright, C.J. (2012). Characterisation and application of a novel positively charged nanofiltration membrane for the treatment of textile industry wastewaters. *Water Research,* 46, 33. DOI: 10.1016/j.watres.2011.10.011

[5] Rahimi, R., Kerdari, H., Rabbani, M., Shafiee, M. (2011). Synthesis, characterization and adsorbing properties of hollow Zn-Fe_2O_4 nanospheres on removal of Congo red from aqueous solution. *Desalination,* 280, 412. DOI: 10.1016/j.desal.2011.04.073

[6] Afkhami, A., Moosavi, R. (2010). Adsorptive removal of Congo red, a carcinogenic textile dye, from aqueous solutions by maghemite nanoparticles. *Journal of Hazardous Materials*, 174, 398. DOI: 10.1016/j.jhazmat.2009.09.066

[7] Hassani, A., Krishnan, S., Scaria, J., Eghbali, P., Nidheesh, P. (2021). Z-scheme photocatalysts for visible-light-driven pollutants degradation: A review on recent advancements. *Current Opinion in Solid State & Materials Science,* 25, 100941. DOI: 10.1016/j.cossms.2021.100941

[8] Karim, A., Hassani, A., Scaria, J., Eghbali, P., Nidheesh, P., (2022). Nanostructured modified layered double hydroxide (LDHs)- based catalysts: A review on synthesis, characterization,and applications in water remediation by advanced oxidation processes. *Current Opinion in Solid State & Materials Science,* 26, 100965. DOI: 10.1016/j.cossms.2021.100965

[9] Reddy, C., Babu, V.B., Shim, J. (2018). Synthesis, optical properties and efficient photocatalytic activity of CdO/ZnO hybrid nanocomposite. *Journal of Physics and Chemistry of Solids,* 112, 20-28. DOI: 10.1016/j.jpcs.2017.09.003

[10] Madihi-Bidgoli, S., Asadnezhad, S., Nezhad, A., Hassani, A., (2021). Azurobine degradation using Fe_2O_3@multi-walled carbon nanotube activated peroxymonosulfate (PMS) under UVA-LED irradiation: performance, mechanism and environmental application. *Journal of Environmental Chemical Engineering,* 9, 106660. DOI: 10.1016/j.jece.2021.106660

[11] Vaizoğullar, A. (2018). Needle-Like La-Doped MgOPhotocatalyst: Synthesis, Characterization and Photodegradation of Flumequine Antibiotic Under UV Irradiation. *Journal of Electronic Materials*, 47, 6751–6758. DOI: 10.1007/s11664-018-6591-0

[12] Wang, G., Gang, L., Li, Z., Wang, B., Zhang, W., Yuan, B., Zhou, T., Long, X., Kuang, A. (2020). Two–dimensional CdO/CdS heterostructure used for visible light photocatalysis. *Physical Chemistry Chemical Physics*, 22, 9587-9592. DOI: 10.1039/D0CP00876A

[13] Tadjarodi, A., Imani, M. (2011). A novel nanostructure of cadmium oxide synthesized by mechanochemical method. *Materials Research Bulletin*, 46, 1949. DOI: 10.1016/j.materresbull.2011.07.016

[14] Ren, H.X., Huang, X.J., Yarimaga, O., Choi, Y.K., Gu, N. (2009). A cauliflower-like gold structure for superhydrophobicity. *Journal of Colloid and Interface Science,* 334, 103. DOI: 10.1016/j.jcis.2009.03.023

[15] Rajeshwar, K., Osugi, M.E., Chanmanee, W., Chenthamarakshan, C.R., Zanoni, M.V.B., Kajitvichyanukul, K., Krishnanayer, P.R. (2008). Heterogeneous photocatalytic treatment of organic dyes in air and aqueous media. *Journal of Photochemistry and Photobiology C: Photochemistry Reviews,* 9, 171. DOI: 10.1016/j.jphotochemrev.2008.09.001

[16] Ghoshal, T., Kar, S., De, S.K. (2009). Morphology controlled solvothermal synthesis of $Cd(OH)_2$ and CdO micro/nanocrystals on Cd foil Morphology. *Applied Surface Science,* 255, 8091-8097. DOI: 10.1016/j.apsusc.2009.05.021

[17] Gulino, A., Compagnini, G., Scalisi, A.A. (2003). Large Third-Order Nonlinear Optical Properties of Cadmium Oxide Thin Films. *Chemistry of Materials*, 15(17), 3332–3336. DOI: 10.1021/cm031075f

[18] Yakuphanoglu, F. (2010). Nanocluster n-CdO thin film by sol–gel for solar cell applications. *Applied Surface Science,* 257(5), 1413-1419. DOI: 10.1016/j.apsusc.2010.08.045

[19] Desai, S.P., Suryawanshi, M.P., Bhosale, S.M., Kim, J.H., Moholkar, A.V. (2015). Influence of growth temperature on the physicochemical properties of sprayed cadmium oxide thin films. *Ceramics International*, 41(3), 4867-4873. DOI: 10.1016/j.ceramint.2014.12.045

[20] Saha, B., Thapa, R., Chattopadhyay, K.K. (2008). Wide range tuning of electrical conductivity of RF sputtered CdO thin films through oxygen partial pressure variation. *Solar Energy Materials and Solar Cells*, 92(9), 1077-1080. DOI: 10.1016/j.solmat.2008.03.024

[21] Rane, Y.N., Shende, D.A., Raghuwanshi, M.G., Koli, R.R., Gosavi, S.R., Deshpande, N.G. (2018). Visible-light assisted CdO nanowires photocatalyst for toxic dye degradation studies. *Optik*, 179, 535-544. DOI: 10.1016/j.ijleo.2018.10.215

[22] Yadav, A.A., Barote, M.A., Chavan, T.V., Masumdar, E.U. (2011). Influence of indium doping on the properties of spray deposited $CdS_{0.2}Se_{0.8}$ thin films. *Journal of Alloys and Compounds,* 509(3), 916–921. DOI: 10.1016/j.jallcom.2010.09.130

[23] Millesi, S., Schilirò, M., Greco, F., Crupi, I., Impellizzeri, G., Priolo, F., Egdell, R.G., Gulino, A. (2016). Nanostructured CdO thin films for water treatments. *Materials Science in Semiconductor Processing*, 42, 85–88. DOI: 10.1016/j.mssp.2015.08.005

[24] Chong, C., Lee, T., Juan, J., Johan, M., Loke, C., Ng, K., Lai, J., Lim, T. (2022). Superparamagnetic Iron Oxide Decorated Indium Hydroxide Nanocomposite: Synthesis, Characterization and Its Photocatalytic Activity. *Bulletin of Chemical Reaction Engineering &*

Catalysis, 17(1), 113–126. DOI: 10.9767/bcrec.17.1.12352.113-126

[25] Tharayil, N.J., Raveendran R., Vaidyan, A.V., Chithra, P.G. (2008). Optical, electrical and structural studies of nickel-cobalt oxide nanoparticles. *Indian Journal of Engineering and Materials Sciences*, 15, 489-496.

[26] Bulakhe, R.N., Lokhande, C.D. (2013). Chemically deposited cubic structured CdO thin films: Room temperature. *AIP Conference Proceedings*, 1536, 503. DOI: 10.1063/1.4810321

[27] Saleh, T.A., Gupta, V.K. (2012). Photocatalyzed degradation of hazardous dye methyl orange by use of a composite catalyst consisting of multi-walled carbon nanotubes and titanium dioxide. *Journal of Colloid and Interface Science,* 371, 101-106. DOI: 10.1016/j.jcis.2011.12.038

[28] Şakar, B.C., Saritaş, S., Kundakçi, M. (2021). Comparison of the optical and morphological properties of CdO thin films obtained by different methods. *Materials Today: Proceedings*, 46, 6888-6891. DOI: 10.1016/j.matpr.2021.01.551

[29] Liu, X., Li, K., Wu, C., Zhou, Y., Pei, C. (2014). Egg white-assisted preparation of inorganic functional materials: A sustainable, eco-friendly, low-cost and multifunctional method. *Ceramics International*, 45(18), 23869-23889. DOI: 10.1016/j.ceramint.2019.08.152

[30] Singh, J., Kumar, P., Hui, K.S., Hui, K.N., Raman, K., Tiwari, R.S., Srivastava, O.N. (2012). Synthesis, band-gap tuning, structural and optical investigations of Mg doped ZnO nanowires. *CrystEngComm*, 14(18), 5898-5904. DOI: 10.1039/C2CE06650E

[31] Zandi, S., Kameli, P., Salamati, H., Ahmadvand, H., Hakimi, M. (2011). Microstructure and optical properties of ZnO nanoparticles prepared by a simple method. *Physica B: Condensed Matter*, 406 (17), 3215-3218. DOI: 10.1016/j.physb.2011.05.026

[32] Malecka, B., Lacz, A. (2008). Thermal decomposition of cadmium formate in inert and oxidative atmosphere. *Thermochim Acta,* 479 (1-2), 12-16. DOI: 10.1016/j.tca.2008.09.003

[33] Ren, W., Ai, Z., Jia, F., Zhang, L., Fan, X., Zou, Z. (2007). Low temperature preparation and visible light photocatalytic activity of mesoporous carbon-doped crystalline TiO_2. *Applied Catalysis B: Environmental*, 69, 138-144. DOI: 10.1016/j.apcatb.2006.06.015

[34] Dhas, C.R., Venkatesh, R., Jothivenkatachalam, K., Nithya, A., Benjamin, B.S., Raj, A.M.E., Jeyadheepan, K., Sanjeeviraja, C. (2015). Visible light driven photocatalytic degradation of Rhodamine B and Direct Red using cobalt oxide nanoparticles. *Ceramics International*, 3, 238. DOI: 10.1016/j.ceramint.2015.03.238

[35] Ngan, T., Thuy, T., Tan, L., Nguyen, T. (2021) Iron-Manganese Bimetallic-Organic Framework as a Photocatalyst for Degradation of Rhodamine B Organic Dye Under Visible Light. *Bulletin of Chemical Reaction Engineering & Catalysis,* 16(4), 916-924. DOI: 10.9767/bcrec.16.4.11764.916-924

[36] Azadeh, T., Mina, I., Hamed, K. (2013). Experimental design to optimize the synthesis of CdO cauliflower-like nanostructure and high performance in photodegradation of toxic azo dyes. *Materials Research Bulletin,* 48 (3), 935-942. DOI: 10.1016/j.materresbull.2012.11.042

[37] Kottam, N., Girija, C.R., Nagabhushana, B.M. (2012). Photocatalytic degradation of Rhodamine B dye under UV/solar light using ZnO nanopowder synthesized by solution combustion route. *Powder Technology*, 215, 91-97. DOI: 10.1016/j.powtec.2011.09.014

[38] Natarajan, K., Natarajan, T.S., Bajaj, H.C., Tayade, R.J. (2011). Photocatalytic reactor based on UV-LED/TiO_2 coated quartz tube for degradation of dyes. *Chemical Engineering Journal*, 178, 40. DOI: 10.1016/j.cej.2011.10.007

[39] Ghorai, T. K., Chakraborty, M., Pramanik, P., (2011). Photocatalytic performance of nanophotocatalyst from TiO_2 and Fe_2O_3 by mechanochemical synthesis. *Journal of Alloys and Compounds,* 509, 8158. DOI: 10.1016/j.jallcom.2011.05.069

[40] El-Morsi, T.M., Budakowski, W.R., Abd-El-Aziz, A.S., Friesen, K.J. (2000). Photocatalytic Degradation of 1,10-Dichlorodecane in Aqueous Suspensions of TiO_2: A Reaction of Adsorbed Chlorinated Alkane with Surface Hydroxyl Radicals. *Environmental Science & Technology*, 34, 1018-1022. DOI: 10.1021/es9907360

[41] Thein, M.T., Pung, S.Y., Chim, J.E., Pung, Y.F. (2017). Highly UV light driven WOx @ ZnO nanocomposites synthesized by liquid impregnation method. *Journal of Industrial and Engineering Chemistry*, 46, 119-129. DOI: 10.1016/j.jiec.2016.10.022